Research Article | Vol. 8, No. 4 | 1 Apr 2018 | OPTICAL MATERIALS EXPRESS 1069
Optical Materials EXPRESS

Graphene-based tunable plasmon induced transparency in gold strips

Mohsin Habib,[1,2,5] Alireza Rahimi Rashed,[1,3] Ekmel Ozbay,[1,2,4] and Humeyra Caglayan[3,*]

[1] *Department of Electrical and Electronics Engineering, Bilkent University, Ankara 06800, Turkey*
[2] *Nanotechnology Research Center, Bilkent University, Ankara 06800, Turkey*
[3] *Laboratory of Photonics, Tampere University of Technology, 33720 Tampere, Finland*
[4] *Department of Physics, Bilkent University, Ankara 06800, Turkey*
[5] *mohsin.habib@bilkent.edu.tr*
[*] *humeyra.caglayan@tut.fi*

Abstract: Plasmon induced transparency (PIT) has been numerically investigated and experimentally realized by two parallel gold strips on graphene for the mid-infrared (MIR) range. The PIT response is realized by the weak hybridization of two bright modes of the gold strips. The response of the device is adjusted with the lengths of two strips and tuned electrically in real time by changing the Fermi level (E_f) of the graphene. E_f is changed to tune the resonance frequency of the transparency window. A top gating is used to achieve high tunability and a 263 nm shift is obtained by changing the gate voltage from -0.6 V to 2.4 V. The spectral contrast ratio of our devices is up to 82%.

OCIS codes: (250.5403) Plasmonics; (240.6680) Surface plasmons.

References and links

1. K. J. Boller, A. Imamoglu, and S. E. Harris, "Observation of electromagnetically induced transparency," Phys. Rev. Lett. **66**(20), 2593–2596 (1991).
2. J. P. Marangos, "Topical review electromagnetically induced transparency," J. Mod. Opt. **45**(3), 471–503 (1998).
3. A. Kasapi, M. Jain, G. Y. Yin, and S. E. Harris, "Electromagnetically induced transparency: propagation dynamics," Phys. Rev. Lett. **74**(13), 2447–2450 (1995).
4. S. E. Harris, J. E. Field, and A. Kasapi, "Dispersive properties of electromagnetically induced transparency," Phys. Rev. A **46**(1), R29–R32 (1992).
5. T. F. Krauss, "Why do we need slow light?" Nat. Photonics **2**(8), 448–450 (2008).
6. M. Fleischhauer, A. Imamoglu, and J. P. Marangos, "Electromagnetically induced transparency: Optics in coherent media," Rev. Mod. Phys. **77**(2), 633–673 (2005).
7. R. D. Kekatpure, E. S. Barnard, W. Cai, and M. L. Brongersma, "Phase-coupled plasmon induced transparency," Phys. Rev. Lett. **104**(24), 243902 (2010).
8. Y. Wu, J. Saldana, and Y. Zhu, "Large enhancement of four-wave mixing by suppression of photon absorption from electromagnetically induced transparency," Phys. Rev. A **67**(1), 013811 (2003).
9. V. Yannopapas, E. Paspalakis, and N. V. Vitanov, "Electromagnetically induced transparency and slow light in an array of metallic nanoparticles," Phys. Rev. B **80**(3), 035104 (2009).
10. C. Rohde, K. Hasegawa, and M. Deutsch, "Plasmon-assisted transparency in metal-dielectric microspheres," Opt. Lett. **32**(4), 415-417 (2007).
11. Y. A. Vlasov, M. O. Boyle, H. F. Hamann, and S. J. McNab, "Active control of slow light on a chip with photonic crystal waveguides," Nature **438**(7064), 65–69 (2005).
12. J. Xie, X. Zhu, X. Zang, Q. Cheng, Y. Ye, and Y. Zhu, "High extinction ratio electromagnetically induced transparency analogue based on the radiation suppression of dark modes," Sci. Rep. **7**(1), 11291 (2017).
13. X. Yan, T. Wang, S. Xiao, T. Liu, H. Hou, L. Cheng, and X. Jiang, "Dynamically controllable plasmon induced transparency based on hybrid metal-graphene metamaterials," Sci. Rep. **7**(1), 13917 (2017).
14. N. Liu, L. Langguth, T. Weiss, J. Kastel, M. Fleischhauer, T. Pfau, and H. Giessen, "Plasmonic analogue of electromagnetically induced transparency at the Drude damping limit," Nat. Mater. **8**(9), 758–762 (2009).
15. S. N. Papasimakis, V. A. Fedotov, N. I. Zheludev, and S. L. Prosvirnin, "Metamaterial analog of electromagnetically induced transparency," Phys. Rev. Lett. **101**(25), 253903 (2008).
16. P. Tassin, L. Zhang, T. Koschny, E. N. Economou, and C. M. Soukoulis, "Low-loss metamaterials based on classical electromagnetically induced transparency," Phys. Rev. Lett. **102**(5), 5595–5605 (2009).

#319262 https://doi.org/10.1364/OME.8.001069
Journal © 2018 Received 9 Jan 2018; revised 20 Mar 2018; accepted 23 Mar 2018; published 28 Mar 2018

Optical Materials EXPRESS

17. H. Zhang, Y. Cao, Y. Liu, Y. Li, and Y. Zhang, "A novel graphene metamaterial design for tunable terahertz plasmon induced transparency by two bright mode coupling," Opt. Commun. **391**, 9–15 (2017).
18. H. Zhuang, F. Kong, K. Li, and S. Sheng, "Graphene-based electromagnetically induced transparency with coupling Fabry-Perot resonators," Appl. Opt. **54**(24), 7455–7461 (2015).
19. X. Shi, D. Z. Han, Y. Y. Dai, Z. F. Yu, Y. Sun, H. Chen, X. H. Liu, and J. Zi, "Plasmonic analog of electromagnetically induced transparency in nanostructure graphene," Opt. Express **21**(23), 28438–28443 (2013).
20. X. Zhao, C. Yuan, L. Zhu, and J. Yao, "Graphene-based tunable terahertz plasmon-induced transparency metamaterial," Nanoscale **8**(33), 15273–15280 (2016).
21. X. Zhou, T. Zhang, X. Yin, L. Chen, and X. Li, "Dynamically tunable electromagnetically induced transparency in graphene-based coupled micro-ring resonators," IEEE Photonics J. **9**(2), 1–9 (2017).
22. H. Zhang, Y. Cao, Y. Liu, Y. Li, and Y. Zhang, "Electromagnetically induced transparency based on cascaded pi-shaped graphene nanostructure," Plasmonics **12**(6), 1833–1839 (2016).
23. K. S. Novoselov, A. K. Geim, S. V. Morozov, D. Jiang, M. I. Katsnelson, I. V. Grigorieva, S. V. Dubonos, and A. A. Firsov, "Two-dimensional gas of massless Dirac fermions in graphene," Nature **438**(7065), 197–200 (2005).
24. K. S. Novoselov, A. K. Geim, S. V. Morozov, D. Jiang, Y. Zhang, S. V. Dubonos, I. V. Grigorieva, and A. A. Firsov, "Electric field effect in atomically thin carbon films," Science **306**(5696), 666–669 (2004).
25. A. K. Geim, and K. S. Novoselov, "The rise of graphene," Nat. Mater. **6**(3), 183–191 (2007).
26. N. Papasimakis, Z. Luo, Z. X. Shen, F. D. Angelis, E. D. Fabrizio, A. E. Nikolaenko, and N. I. Zheludev, "Graphene in a photonic metamaterial," Opt. Express **18**(8), 8353–8359 (2010).
27. Y. Zou, P. Tassin, T. Koschny, and C. M. Soukoulis, "Interaction between graphene and metamaterials: split rings vs. wire pairs," Opt. Express **20**(11), 12198–12204 (2012).
28. S. Xiao, T. Wang, Y. Liu, C. Xu, X. Han, and X. Yan, "Tunable light trapping and absorption enhancement with graphene ring arrays," Phys. Chem. Chem. Phys. **18**(38), 26661–26669 (2016).
29. H. Li, L. Wang, and X. Zhai, "Tunable graphene-based mid-infrared plasmonic wide-angle narrowband perfect absorber," Sci. Rep. **6**(1), 36651 (2016).
30. S. Xiao, T. Wang, X. Jiang, X. Yan, L. Cheng, B. Wang, and C. Xu, "Strong interaction between graphene layer and Fano resonance in terahertz metamaterials," J. Phys. D: Appl. Phys. **50**(19), 195101 (2017).
31. P. Tassin, T. Koschny, and C. M. Soukoulis, "Graphene for terahertz applications," Science **341**(6146), 620–621 (2013).
32. S. Cakmakyapan, H. Caglayan, and E. Ozbay, "Coupling enhancement of split ring resonators on graphene," Carbon **80**, 351–355 (2014).
33. K. F. Mak, L. Ju, F. Wang, and T. F. Heinz, "Optical spectroscopy of graphene: from the far infrared to the ultraviolet," Solid State Comm. **152**(15), 1341–1349 (2012).
34. Z. Q. Li, E. A. Henriksen, Z. Jiang, Z. Hao, M. C. Martin, P. Kim, H. L. Stormer, and D. N. Basov, "Dirac charge dynamics in graphene by infrared spectroscopy," Nat. Phys. **4**(7), 532–535 (2008).
35. V. E. Dorgan, M. H. Bae, and E. Pop, "Mobility and saturation velocity in graphene on SiO_2," Appl. Phys. Lett. **97**(8), 082112 (2010).
36. H. H. Li, "Refractive index of alkaline earth halides and its wavelength and temperature derivatives," J. Phys. Chem. Ref. Data **9**(1), 161–290 (1980).
37. O. Ozdemir, A. M. Aygar, O. Balci, C. Kocabas, H. Caglayan, and E. Ozbay, "Enhanced tunability of V-shaped plasmonic structures using ionic liquid gating and graphene," Carbon **108**, 515–520 (2016).
38. A. M. Aygar, S. Cakmakyapan, O. Balci, C. Kocabas, H. Caglayan, and E. Ozbay, "Comparison of back and top gating schemes with tunable graphene fractal metasurfaces," ACS Photonics **3**(12), 2303–2307 (2016).

1. Introduction

Electromagnetically induced transparency (EIT) is a phenomenon that reduces the absorption of an optically thick medium over a narrow spectrum by the quantum interference effect [1–4]. This can be used for slow light applications [5], optical switching [6], quantum information processing [6], optical storage [7], and nonlinear optical enhancement [8]. A plasmonic analogue of EIT has been observed in metallic nanoparticles [9, 10], integrated photonic structure [11], metamaterial structures [12–16] and is known as plasmon induced transparency (PIT). In most of these studies, PIT has been investigated by the destructive interference of dark-bright modes and detuning of two bright modes. In destructive interference, there is a coherent coupling between narrow and broad band resonances of two dipole antennas [14]. Another way to obtain PIT is the weak hybridization of two bright modes having different resonances due to different dimensions [17]. Dynamically tunable PIT can offer promising applications, such as electrically switchable camouflage systems and tunable enhanced sensing.

Recently, tunable PIT has been numerically investigated by several groups. Their designs are

Optical Materials EXPRESS

either based on graphene structures, such as Fabry-Perot resonators [18,19], ring resonators [20,21], and cascaded pi-shaped structures [22], or on hybrid metal-graphene metamaterials [13]. However, the successful realization of these numerical investigations has not been achieved due to the fabrication difficulties of the suggested structures. Graphene based structures require high quality graphene layer on substrates without any cracks, which is limited by transfer methods. Therefore, hybrid metamaterials are an efficient strategy to realize tunable PIT. We have experimentally demonstrated dynamically tunable PIT with simple gold (Au) strips on graphene. By modifying the lengths of Au strips we are able to adjust the PIT response of the device. Moreover, our design allows us to electrically tune the response of device in real time by changing the Fermi level (E_f) of graphene.

Graphene is a single atomic layer thick material (2-D Material) in which carbon atoms form a honeycomb lattice [23], discovered by Novoselov *et al.* in 2004 [24]. Graphene has remarkable properties, which has made it an active research area for the last decade [25–27]. At mid-infrared (MIR) graphene has tight field confinement [28] and a controllable E_f with gate voltage [29–32], which makes graphene a suitable candidate for tuning resonances electrically. The interaction of light with graphene can be explained by the concept of Pauli Blocking [33], as graphene forms a conical band diagram. There are two types of transition(s) in graphene depending upon the energy of the photons: the two transitions are actually always present regardless of the photon energy. However, when the energy is less than $2E_f$ the intra-band transition is dominant and if the energy is higher than $2E_f$ the inter-band becomes dominant. Devices with high tunability mostly operate near $2E_f$ [34]. Graphene E_f is a direct function of charge density as shown in Equation 1. Where $\hbar$ is reduced Planck's constant, n is charge density and v_F is Fermi velocity that is -1.1× 10^8 cm s^{-1} [35].

$$E_f = \hbar v_F \sqrt{\pi n} \tag{1}$$

The surface conductivity of graphene can be changed by a variety of gating methods, and results in the change of E_f that can be used to tune the optical response of plasmonic structures on graphene. Falkovsly presented a mathematical model for the surface conductivity of graphene as:

$$\sigma(\omega) = \frac{e^2\omega}{i\pi\hbar}\left[\int_{-\infty}^{+\infty}\frac{|\epsilon|}{\omega^2}\frac{df_0(\epsilon)}{d\epsilon}d\epsilon - \int_0^{+\infty}\frac{f_0(-\epsilon)-f_0(\epsilon)}{(\omega+i\delta)^2-4\epsilon^2}d\epsilon\right] \tag{2}$$

where complex conductivity (σ) is a function of frequency (ω) and Fermi function $f_0(\epsilon)$= $\{\exp[(\epsilon\text{-}\mu_c)/(k_BT)]+1\}^{-1}$, ($k_B$ is Boltzmann's constant). In these equations, intra-band electron photon scattering, and inter-band electron transitions are represented by first and second terms, respectively. Integrating the first term leads to equation 3 which shows the intra-band conductivity of graphene. In the second term, where $\delta\rightarrow 0$ is the infinitesimal quantity determining the bypass around the integrand pole, owes its origin to the direct inter-band electron transitions.

$$\sigma^{intra}(\omega) = \frac{2ie^2T}{\pi\hbar(\omega+i\tau^{-1})}ln\left[2cosh\left(\frac{\mu_c}{2T}\right)\right] \tag{3}$$

In equation 3, μ_c is chemical potential, τ is scattering time, and T is temperature, as the graphene chemical potential can be controlled by gating and therefore graphene is highly tunable by gating in intra-band region.

2. Method

We have investigated and realized two parallel Au strips on graphene with BaF_2 substrate as shown in Fig. 1. Each of these strips has their own plasmonic resonance that serves as two different bright modes. The detuning of these bright modes creates a PIT response in the MIR region, which is tuned by changing E_f of graphene. First, we numerically investigated the tunable PIT

Optical Materials EXPRESS

using the Finite Difference Time-Domain (FDTD) method in commercially available software (Lumerical FDTD Solutions). The unit cell of the design as shown in Fig. 1(a) has periodic boundaries along the x and y-axes and Perfect Matched Layers (PML) in the z-axis (propagation direction). Two devices are investigated with different lengths of strips, L1 & L2, which are selected as 3.2 & 2.4 μm for the first device and 3.4 & 2.6 μm for the second device, respectively. However, the thickness (T=70 nm), width (W= 0.5 μm), and distance (D= 0.2 μm) between the two strips are kept constant in both of the devices. Graphene is introduced as a 2D dispersive material between the BaF_2 and the Au strips. In our calculations, the optical constant of the gold is considered based on Palik model and the applied optical parameters of the BaF_2 is extracted from Reference [36]. The unit cell is illuminated by a plane wave source along the z direction having electric component (E) parallel to x-axis. Scattering rate of graphene was set as 0.01 eV (2.4×10^{12} sec^{-1}), T was set as 300 K and μ_c was changed from 0.5 eV to 0.8 eV, which matches the experimental results from -0.6 V to 2.4 V and are consistent with previous studies [37, 38].

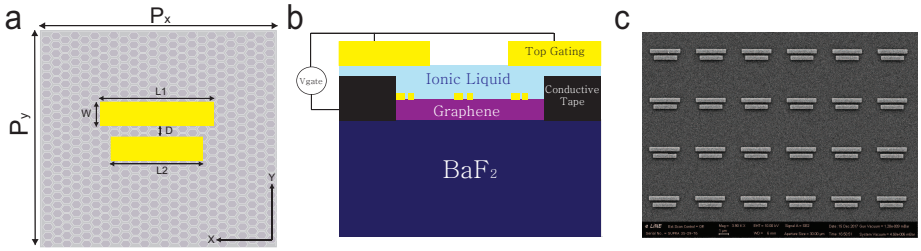

Fig. 1. (a) Unit cell of PIT structure. Two Au strips (golden) with lengths of L1 and L2 on graphene (grey) are presented. Two devices are designed with two different lengths of strips. Px and Py show periodicity of unit cell. (b) Schematic of ionic gating of PIT device. Two BaF_2 substrates are used. The first one with Au strips on graphene (purple), which is connected to the source by conductive tape (black). The second one with a window for FTIR measurements and coated with Ti/Au (golden), which is connected to second terminal of the source. Ionic liquid (light blue) is injected between these two substrates. (c) SEM image of PIT structure.

The device was fabricated based on simulation design, using a commercially available chemical vapor deposition (CVD) grown graphene on Cu. The graphene was transferred onto BaF_2 substrates by the wet transfer method and spin coated with positive photo resist (PMMA A4) and aqua save. Coated sample was exposed to a dose of 2000 pC/cm^2 under E-beam to form strips. The exposed samples were developed in a developer (MIBK: IPA) for 1 minute. 5/65 nm of Ti/Au were deposited by E-beam evaporator at constant rate (1 Å/sec) for both metals, structures appeared after the lift-off process of 24 hours in acetone. An SEM image of a fabricated device is shown in Fig. 1(c). In order to apply voltage to the graphene, the top gating method was used [37, 38]. For this, we used other BaF_2 substrates with metal contacts at the corners and a transparent window at the center, formed by photolithography. Contact with graphene is made using conductive tape. An Ionic liquid (Diethylmethyl(2-methoxyethyl) ammonium bis(trifluoromethylsulfonyl) imide, [deme][Tf2N]) was inserted between two substrates which were insulated by tape. A schematic is shown by Fig. 1(b). Ionic liquid is used for low operational voltage, in which ions accumulate at the surface of graphene and change the E_f of graphene.

Normalized transmission measurements for two different devices were obtained by using a Fourier transform infrared (FTIR) instrument integrated with microscope. Measurements were done from 6 to 14 μm at different gate voltage using the ionic gating. By changing the gate voltage surface carrier concentration, E_f of graphene was observed in PIT phenomenon. For the measurement, samples were illuminated by x polarized field. The background measurements were taken from graphene on BaF_2 substrates with no PIT structures.

Optical Materials EXPRESS

3. Results and discussion

The transmission simulation for each of the Au strips shows strong responses as presented in the insets of Fig. 2(a) and 2(b). As described above, when we bring two strips close to each other, they result in a weak hybridization and give the PIT response presented in Fig. 2(a) and 2(b). This response is not observed by the excitation of single strip. By carefully designing the lengths and distance between the strips, we investigated the PIT phenomenon for two different strips. Furthermore, this PIT response was tuned by changing E_f of graphene in simulations presented in Fig. 2(a) and 2(b). This response is shifted toward shorter wavelengths as E_f of graphene is increased from 0.5 eV to 0.8 eV. For reflection and absorption results of shorter dimension at 0.5 eV see Appendix A. Fig. 2(c) shows the measured transmission of the device with shorter lengths of strips (3.2 and 2.4 μm), SEM image shown in the inset. Similarly measured transmission of the device with a longer dimension of strips (3.4 and 2.6 μm) is presented in Fig. 2(d), with an SEM image in the inset. As the gate voltage is increased from -0.6 V to 2.4 V, a blue shift is observed in PIT for both devices. We have observed good agreement with simulations for changing E_f from 0.5 eV to 0.8 eV. The minimum gate voltage was selected based on charge neutrality point (CNP), measured previously to be -0.6 V for a similar graphene structure [37, 38].

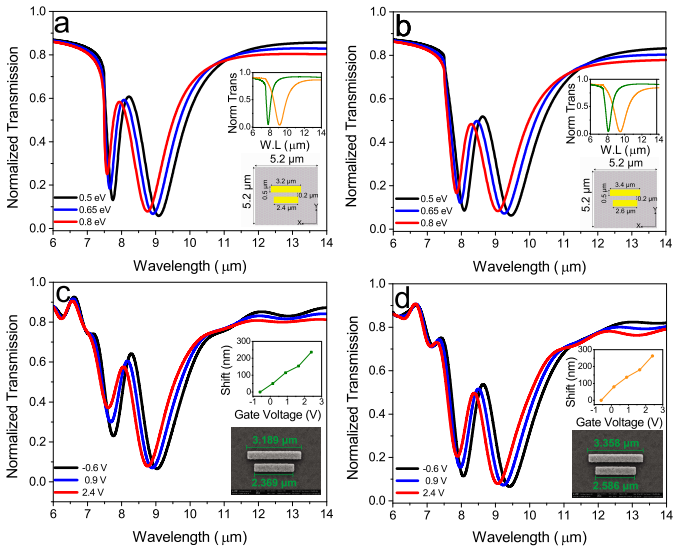

Fig. 2. Simulated and FTIR measurement of PIT structures. Simulated results of (a) shorter dimension and (b) longer dimension for different E_f. Normalized transmission for (c) shorter dimension and (d) longer dimension at -0.6 V, 0.9 V and 2.4 V, SEM image with dimension in the inset.

Total shift of 235 nm was observed for shorter dimension and 263 nm for longer dimension by changing gate voltage of 3.0 V. Shift in PIT transmission peak at the applied gate voltage with respect to CNP is obtained for both the devices and shown in the insets of Fig. 2(c) and 2(d). Investigation of E-field for two strips that resulted in resonances at different wavelengths is investigated for a device with shorter dimensions (Fig. 3). Electric field magnitudes of two resonance wavelengths in the transmission spectrum (7.75 μm and 9.06 μm) is shown in Fig. 3(a) and 3(c). In addition, the E-field magnitude at a PIT wavelength is shown in Fig. 3(b). These results show that each of the strips are excited separately at the resonance wavelengths and act as bright mode resonances. However, at 8.22 μm, both strips are excited simultaneously resulting in the PIT phenomenon. Major localization is at the corner of the strips at their own resonance wavelengths and between two strips for transmission peak of PIT. Spectral contrast ratio (S_{con}) is

Optical Materials EXPRESS

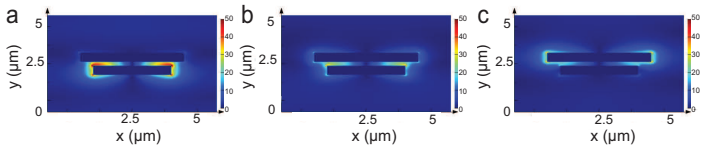

Fig. 3. E-field magnitude at 0.5 eV for (a) 7.75 μm. (b) 8.22 μm (c) 9.06 μm.

used to evaluate the performance of PIT response in optical applications [13] and described as:

$$S_{\text{con}} = \frac{(T_{\text{peak}} - T_{\text{dip}})}{(T_{\text{peak}} + T_{\text{dip}})} \times 100 \tag{4}$$

where T_{peak} is intensity of transmission peak and T_{dip} is intensity of resonance dip. Spectral contrast ratios of our devices are 82% and 78% for shorter and longer dimensions, respectively. Both devices with a high spectral contrast ratio and high tunability are suitable for filtering and switching applications.

4. Conclusion

In this work, tunable PIT devices are numerically investigated and experimentally realized. Resonance frequencies of two strips were tailored by adjusting the length of the strips and tuned by changing the E_f of graphene layer. A large tuning range was demonstrated for the FTIR measurements of PIT structures by applying gate voltage. We were able to obtain 263 nm of shift in transmission window by applying gate voltage from -0.6 V to 2.4 V. This concept of real time tuning PIT is exciting for novel devices in the field of optical switching, modulation, slow light applications, tunable sensors, filters, photoluminescence, and enhancing nonlinear interactions.

Appendix A: Simulation results of reflection and absorption

As it is evident from the presented simulation results in Fig. 4, in the designed structure the resonances of PIT response are compensated by both reflection and absorption peaks.

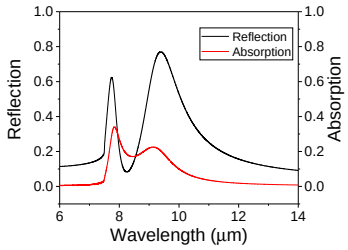

Fig. 4. Simulation results of reflection and absorption at 0.5 eV for shorter dimension.

Funding

Academy of Finland, Competitive Funding to Strengthen University Research Profiles (301820).

Acknowledgements

The authors acknowledge O. Ozdemir for sharing useful information. E.O. acknowledges the partial support from the Turkish Academy of Sciences.